

# Calculations on the Electronic Structure and UV–Visible Spectrum of Oxyhemocyanin

Guillermina Lucia Estiú<sup>†</sup> and Michael C. Zerner<sup>\*\*‡</sup>

Contribution from the Departamento de Química, CEQUINOR, Facultad de Ciencias Exactas, Universidad Nacional de La Plata, C.C. 962-1900 La Plata, Argentina, and Quantum Theory Project, University of Florida, Gainesville, Florida 32611

Received April 17, 1997. Revised Manuscript Received November 2, 1998

**Abstract:** The ground-state electronic structure and UV–visible spectra of models for oxyhemocyanin are examined using the intermediate neglect of differential overlap model and multireference configuration interaction. The experimental features are interpreted as excitations involving the d orbitals of the Cu atoms and the valence orbitals of the peroxide bridge through which they are antiferromagnetically (AF) coupled. Our model, which replaces the histidine residues with imidazoles, reproduces correctly the higher stability of the AF singlet state and the major spectroscopic features. We examine in detail the geometry of the central part of the molecule, responsible for the activity, using the experimental electronic spectrum as a guide. We further examine the effect that deprotonation of the chelating imidazoles has on the predicted spectroscopy. The central structure that we assumed to best reproduce the spectroscopy is very similar to that obtained from BLYP density functional calculations. For comparison with other results, we also examine a model compound in which NH<sub>3</sub> replaces histidine. For both the imidazole- and the NH<sub>3</sub>-based models, the [Cu<sub>2</sub>(μ-η<sup>2</sup>:η<sup>2</sup>-O<sub>2</sub>)]<sup>2+</sup> and [Cu<sub>2</sub>(η-O)<sub>2</sub>]<sup>2+</sup> isomers have been considered and the results compared with available data. We conclude with the observation that the electronic structure of these compounds does depend on the redox properties of the chelating nitrogen ligands.

## 1. Introduction

Metal–metal interactions have elicited interest among inorganic and bio-inorganic chemists due to their presence in many areas of technology and biology. Ferromagnetic (FM) and antiferromagnetic (AF) couplings between transition metal atoms can be established by selecting an appropriate atomic or molecular bridge for a given pair of metal atoms. It is now possible to design new materials with specific magnetic properties.<sup>1,2</sup> Significant knowledge on these topics has been derived from the study of enzymes, where different electronic interactions appear between the metal atoms that define the receptor site and electron-transfer centers.

Metalloproteins have, in general, homodinuclear active sites involving the first-row transition metal atoms Fe,<sup>3,4</sup> Co,<sup>5</sup> Zn,<sup>6</sup> and Cu,<sup>7</sup> although heterobimetallic active sites have been also found in several important enzymes.<sup>8</sup> A typical example of the first case is given by oxyhemocyanin, a binuclear copper protein present in mollusks and arthropods, generated by reversible

binding of dioxygen to the active site of hemocyanin and centrally involved in oxygen transport. In addition to its biological importance, the structure shows particular magnetic characteristics: EXAFS and EPR spectroscopies have demonstrated that the Cu atoms, in Cu(II) oxidation state, are antiferromagnetically coupled through a peroxide to form singlet and triplet states, the first more than 600 cm<sup>-1</sup> lower in energy than the second.<sup>7,9</sup>

Spectroscopy has played a major role in developing our understanding of the active sites in copper proteins. The blue copper proteins, coupled binuclear copper proteins, and multi-copper oxidases have quite unusual spectral features relative to those of normal copper complexes.<sup>7</sup> The origin of their unique spectral features defines electronic and geometric requirements which play critical roles in biological functions. An accurate reproduction of the UV–visible spectrum allows one to learn about these requirements, to better understand them, and to design materials that, sharing these characteristics, also share the catalytic properties. This is the subject of this work.

From the crystal structure of the protein,<sup>10</sup> it is known that, in oxyhemocyanin, the O<sub>2</sub> is bound as a peroxide in a side-on bridging (μ-η<sup>2</sup>:η<sup>2</sup>) fashion to the copper(II) ions, coordinated by histidine nitrogens in a close-to-square pyramidal structure. The ground state is diamagnetic and is believed to be strongly antiferromagnetically coupled through the peroxide bridge. This complex possesses an absorption spectrum containing two intense bands, at 580 (ε ≈ 1000 M<sup>-1</sup> cm<sup>-1</sup>) and 350 nm (ε ≈ 20 000 M<sup>-1</sup> cm<sup>-1</sup>).

<sup>†</sup> Universidad Nacional de La Plata.

<sup>‡</sup> University of Florida.

(1) De Munno, G.; Julve, M.; Lloret, F.; Faus, J.; Verdager, M.; Caneschi, A. *Inorg. Chem.* **1995**, *34*, 157.

(2) Holman, T. R.; Wang, Z.; Hendrich, M. P.; Que, L. *Inorg. Chem.* **1995**, *34*, 134.

(3) Rosenzweig, A. C.; Frederick, C. A.; Lippard, S. J.; Nortlund, P. *Nature* **1993**, *366*, 537.

(4) True, A. E.; Scarrow, R. C.; Randall, C. R.; Holz, R. C.; Que, L. *J. Am. Chem. Soc.* **1995**, *115*, 4246.

(5) Roderick, S. L.; Matthews, B. W. *Biochemistry* **1993**, *32*, 3907.

(6) Kim, E. E.; Wyckoff, H. W. *J. Mol. Biol.* **1991**, *218*, 449.

(7) Solomon, E. I.; Baldwin, M. J.; Lowery, M. D. *Chem. Rev.* **1992**, *92*, 521.

(8) Beck, J. L.; McConachie, L. A.; Summors, A. C.; Arnold, W. N.; deJersey, J.; Zerner, B. *Biochim. Biophys. Acta* **1986**, *869*, 61.

(9) Tuczek, F.; Solomon, E. I. *J. Am. Chem. Soc.* **1994**, *116*, 6916.

(10) Ton-That, H.; Magnus, K. A. *J. Inorg. Biochem.* **1993**, *51*, 65.  
Magnus, K. A.; Ton-That, H.; Carpenter, J. E. *Protein: Struct., Funct. Genet.* **1994**, *19*, 302.

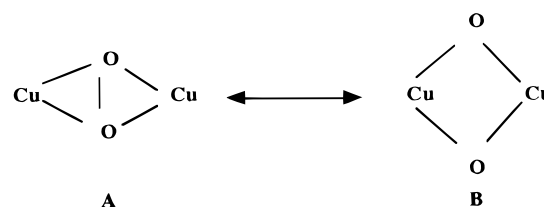
There are several previous theoretical studies on these systems, most occurring very recently. Initial studies are based on spin-restricted broken-symmetry SCF-X $\alpha$ -SW calculations and are limited to model complexes in which the histidine residues were replaced by NH<sub>3</sub>.<sup>11</sup> These studies showed that the key features of the peroxide-copper bond are given by the energies and wave functions of the HOMO and LUMO levels, which are principally metal-centered but also involve the peroxide valence orbitals. The spectroscopic features have been assigned to [O<sub>2</sub>]<sup>2-</sup>  $\pi^* \rightarrow$  Cu(II)(d<sub>x<sup>2</sup>-y<sup>2</sup>) charge-transfer (CT) transitions, for the  $\pi^*$  orbital split in an in-plane, s-bonding orbital,  $\pi^*_{\sigma}$ , and an out-of-plane, p-bonding orbital,  $\pi^*_{\nu}$ . Whereas the band at lower energy, associated with the [O<sub>2</sub>]<sup>2-</sup>  $\pi^*_{\nu} \rightarrow$  Cu(II)(d<sub>x<sup>2</sup>-y<sup>2</sup>) CT transition, was accurately reproduced, the energy of the most intense transition, related to the [O<sub>2</sub>]<sup>2-</sup>  $\pi^*_{\sigma} \rightarrow$  Cu(II)(d<sub>x<sup>2</sup>-y<sup>2</sup>) CT transition, was calculated 30 000 cm<sup>-1</sup> too high in energy.<sup>11</sup> Further valence bond configuration interaction calculations by the same authors, where the data of the previous X $\alpha$  calculations were used as parameters,<sup>9</sup> have lowered the disagreement for the high energy band to 12 000 cm<sup>-1</sup> vs the experimental data, but their conclusions were still based on the analysis of the NH<sub>3</sub>-based model compound.</sub></sub></sub>

Bernardi and co-workers<sup>12</sup> have performed CASSCF, CASPT2, and DFT calculations for smaller model systems of the core Cu<sub>2</sub>O<sub>2</sub> with 3, 2, and no NH<sub>3</sub> chelating ligands. Their CASSCF wave function consists of a heavy mixture of the two reference states, with double occupation of the [d<sub>xy</sub>(a) + d<sub>xy</sub>(b)] (53%) and [d<sub>xy</sub>(a) - d<sub>xy</sub>(b)] (35%) orbitals, which are the HOMO and the LUMO of their calculation, where a and b refer to the two copper atoms. The heavy mixing of these two molecular orbitals (MO) in the resultant wave function indicates antiferromagnetism between two localized d<sub>xy</sub> orbitals (much as such a mixture of states would indicate in the case of the two hydrogen atoms in H<sub>2</sub> at large separation). An interesting conclusion of theirs is that the relative stability of this AF singlet vs the triplet depends on the presence of the NH<sub>3</sub> ligands. These ligands determine the relative energies of the [d<sub>xy</sub>(a) + d<sub>xy</sub>(b)] and [d<sub>xy</sub>(a) - d<sub>xy</sub>(b)] orbitals, and thus the amount of mixing that these orbitals realize with the oxygen  $\pi^*$  orbitals, and eventually in the subsequent correlation treatment.

Cramer, Smith, and Tolman<sup>13</sup> studied the transformation between the [Cu<sub>2</sub>( $\mu$ - $\eta^2$ : $\eta^2$ -O<sub>2</sub>)]<sup>2+</sup> (A) and [Cu<sub>2</sub>( $\mu$ -O<sub>2</sub>)]<sup>2+</sup> (B) complexes that is essential for the functioning of some enzymes.<sup>14</sup> The description of the wave function they obtain is very similar to that found by Bernardi et al. for A, whereas the description for B is considerably more complex, with many dynamic correlating contributions making up some 37% of the wave function. Their results show a very flat surface for this interconversion (Scheme 1).

Recent calculations by Bércecs have shown sensitivity to the nature of the ligands,<sup>15</sup> as did the calculations of Bernardi et al. Bércecs shows that the 1,4,7-triazacyclononane derivatives binds O<sub>2</sub> weakly, and thus likely reversibly, while a hydrotris-(pyrazolyl)borate derivative binds O<sub>2</sub> more strongly and thus, perhaps, irreversibly. The hexaamino complex is not stable

Scheme 1



relative to O<sub>2</sub> dissociation. This binding can also be associated with the ligand field effects described above but are, in fact, analyzed by an energy decomposition scheme of a somewhat different nature. These calculations are of the nonlocal density functional theory (DFT) type and yield a delocalized closed-shell description, although broken symmetry solutions were attempted. This description yields a reasonable singlet-lowest triplet energy difference, but, despite Bércecs's disclaimer, is unlikely to yield the proper electronic spectroscopy, as we examine later in this manuscript.

With the exception of the Solomon work,<sup>9</sup> the previous studies do not deal with the detailed electronic spectroscopy of these compounds.

Because the features that develop in the experimental UV-vis spectra of oxyhemocyanin seem to originate in transitions comprising only the copper atoms and the peroxide through which they are bonded, it becomes evident that detailed structural and electronic characteristics of the central portion of oxyhemocyanin can be obtained from the study of the experimentally observed transitions. Since this site is responsible for the catalytic activity, information on reactivity can also be obtained through the study of the spectrum. We have performed, to this end, semiempirical calculations of the intermediate neglect of differential overlap type, at the multireference configuration interaction level (INDO/S-MRCI). Given an appropriate description of the AF bond, these calculations accurately reproduce the position and intensity of the bands in the UV-vis spectrum. The calculations are not limited to a NH<sub>3</sub>-based model compound but to a model complex closer to that observed in the native enzyme, where the histidine ligands are represented by imidazole groups (Figure 1). The influences of the ligands and the size of the CI in the calculated electronic spectrum are discussed below.

Because of the importance of the transformation shown in Scheme 1 in relation to several biological processes, we have also studied isomer B, both for the imidazole- and NH<sub>3</sub>-based model complexes, at the same level of theory. We have examined the electronic and magnetic properties of the ground state as well as the UV-vis spectroscopy, which is actually known for the 1,4,7-triazacyclononane derivative.<sup>14,16-18</sup>

## 2. Computational Details

The geometry of the oxyhemocyanin molecule is known to a resolution of 1.9 Å from the single-crystal X-ray data of *Limulus polyphemus*.<sup>10</sup> There are six histidine residues coordinating, through the nitrogens, two copper atoms that bind one oxygen molecule. The distance between the copper atoms is 3.6 ± 0.2 Å, while the oxygen atoms are 1.41 Å apart and essentially in the same plane as the copper atoms. Four histidine ligands are closer to the metal centers (~2.00 Å) and almost in the same plane. Both copper atoms are coordinated weakly to a third histidine ligand (2.258 Å),<sup>9</sup> which is placed almost

(11) Ross, P. K.; Solomon, E. I. *J. Am. Chem. Soc.* **1991**, *113*, 3246.

(12) Bernardi, F.; Bottoni, A.; Casadio, R.; Fariselli, P.; Rigo, A. *Int. J. Quantum Chem.* **1996**, *58*, 109.

(13) Cramer, C. J.; Smith, B. A.; Tolman, W. B. *J. Am. Chem. Soc.* **1996**, *118*, 11283.

(14) Halfen, J. A.; Mahapatra, S.; Wilkinson, E. C.; Kaderli, S.; Young, V. G.; Que, L.; Zuberbühler, A. D.; Tolman, W. B. *Science* **1996**, *271*, 1397. Mahapatra, S.; Halfen, J. A.; Wilkinson, E. C.; Pan, G.; Wang, X.; Cramer, C. J.; Tolman, W. B. *J. Am. Chem. Soc.* **1996**, *118*, 11555.

(15) Bércecs, A. *Inorg. Chem.* **1997**, *36*, 4831. Bércecs, A. *Int. J. Quantum Chem.* **1997**, *65*, 1077.

(16) Mahapatra, S.; Halfen, J. A.; Wilkinson, E. C.; Pan, G.; Cramer, C. J.; Que, L.; Tolman, W. B. *J. Am. Chem. Soc.* **1995**, *117*, 8865.

(17) Kitajima, N.; Morooka, Y. *Chem. Rev.* **1994**, *94*, 77.

(18) Solomon, E. I.; Tucze, F.; Root, D. E.; Brown, C. A. *Chem. Rev.* **1994**, *94*, 827.

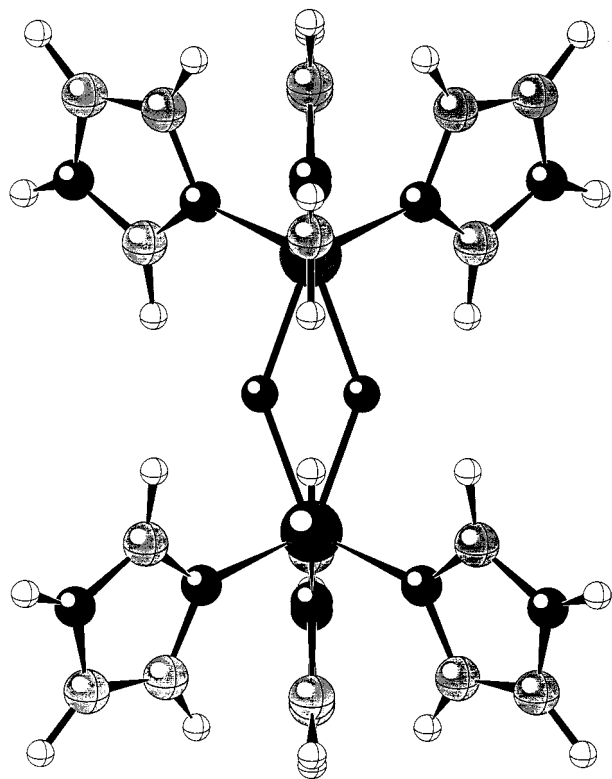


**Figure 1.** Structure of the imidazole-based model of the oxyhemocyanin molecule obtained from the geometry optimization and used in these studies (see text).

axially. Previous calculations on the  $\text{NH}_3$  model compound have assumed either a  $D_{2h}$  structure, neglecting the weakly bonded axial ligands, or a  $C_{2h}$  structure associated with perfectly perpendicular ligands on each Cu atom. However, the angular orientation of the histidine ligands in the biological media is not perfectly known. Moreover, according to the bands that develop in the UV-vis spectrum, an out-of-plane distortion of the oxygen atoms (butterfly distortion)<sup>9</sup> has been inferred. In a first step, we keep the experimental geometry of the central portion and optimize the geometry of the imidazole rings and their orientation relative to it, relaxing also the perpendicularity between the histidine nitrogen atoms. We are aware of the fact that this optimized structure does not have to be the actual one inside the protein, i.e., in the biological media, but, according to the experimental data and from the results of our calculations, should be close enough to be considered an appropriate model for the calculations. Geometry optimizations have been done using the semiempirical AM1 model,<sup>19</sup> as well as a density functional calculation, as will be reported later. In a second step, starting from the experimental data for the central core, the distance between the copper atoms and the out-of-plane shift of the oxygens have been further adjusted by means of single-point calculations using the INDO model,<sup>20–22</sup> parametrized for spectroscopy (INDO/S),<sup>23–25</sup> until optimum agreement between the experimental and calculated UV-vis spectra was achieved. Here we are guided by both the overall appearance of the calculated spectrum and, especially, the lower energy bands that we expect to predict with the greatest accuracy.

The UV-vis spectra have been examined by means of the INDO/S methodology at the configuration interaction singles (CIS) level of

(19) Stewart, J. J. P. *Mopac*, version 7.0; F. J. Seiler Research Laboratory, United States Air Force Academy: Colorado, 1994.

(20) Pople, J. A.; Santry, D. P.; Segal, G. A. *J. Chem. Phys.* **1965**, *43*, S129.

(21) Pople, J. A.; Beveridge, D. L.; Dobosh, P. A. *J. Chem. Phys.* **1967**, *47*, 47.

(22) Zerner, M. C. *ZINDO Package*; Quantum Theory Project: Williamson Hall, University of Florida.

(23) Ridley, J.; Zerner, M. C. *Theor. Chim. Acta* **1973**, *32*, 111.

(24) Ridley, J.; Zerner, M. C. *Theor. Chim. Acta* **1976**, *42*, 223.

(25) Zerner, M. C.; Loew, G.; Kirchner, R.; Mueller-Westerhoff, U. J. *Am. Chem. Soc.* **1980**, *102*, 589.

theory. All self-consistent field (SCF) calculations were of the restricted open-shell Hartree-Fock (ROHF) type, unless otherwise noted.<sup>26</sup> An open-shell operator was defined in order to localize one electron on each copper atom. Localization was achieved by assigning 18 electrons, 16 in the closed-shell and 2 in open-shell orbitals belonging to different copper atoms. The resulting MO distribution was used to compare the stability of the triplet and the AF singlet states. A restricted Hartree-Fock (RHF) procedure was used to calculate the energy of the singlet in a delocalized approach. The SCF calculations were followed by a MRCI treatment, using a Rumer diagram technique<sup>27</sup> for the open-shell structures. Several different CI calculations were performed. A series of smaller calculations, generated from excitations selected from 50 orbitals down and 50 up from the Fermi level, is used to indicate important configurations in the description of the low-lying excited states. The geometry of the central part of the molecule (Cu-Cu and O-O) is inferred from CI calculations including 1145 configurations, a level of CI in which the energy of the low-lying states seems stable. The final calculation used for predicting the spectrum scans all single excitations from the three reference configurations  $S(a)^2$ ,  $S(b)^2$ , and  $S(a)S(b)$ , where the two  $S$  = semioccupied molecular orbitals (SOMO) contain two electrons and are mostly  $d_{xy}$  localized on atom a or b. This scanning selects all those configuration state functions (CSFs) with diagonal excitations less than 60 000  $\text{cm}^{-1}$  above the lowest reference, the  $P'$  space, and then all those CSFs that have a second-order energy contribution to any of the  $P'$  space greater than 10  $\text{cm}^{-1}$ , defining the total  $P$  space. This includes some 6100 CSFs. Oscillator strengths were evaluated with the dipole-length operator,<sup>28</sup> retaining all one-center terms.

To compare our results with the data previously published by Tuczek and Solomon,<sup>9</sup> similar calculations were performed for a model compound in which the histidine residues were replaced by  $\text{NH}_3$  groups. For this smaller compound, the influence of the size of the CI has been also analyzed, comparing a space of 30 orbitals down and 10 up, 1200 configurations, with a smaller CI, comprising 5 orbitals up and 570 configurations.

For both the imidazole- and the  $\text{NH}_3$ -based models, calculations have been extended to isomer B (Scheme 1). Keeping the geometry of the ligands to the one used for isomer A, the coordinates of the central portion have been adjusted to the experimental X-ray data, i.e., Cu-Cu distances of 2.796 Å and O-O distances of 2.29 Å have been used.<sup>14</sup>

### 3. Results and Discussion

**3.1. Ground-State Properties. Magnetism. 3.1.a. Imidazole-Based Model Complex. Isomer A.** It is known from experimental data on the oxyhemocyanin molecule that, upon  $\text{O}_2$  binding, an electron transfer takes place from the two Cu(I) cations to the  $\text{O}_2$ , giving rise to two Cu(II) ions that are strongly AF coupled through the peroxide bridge (coupling constant,  $-2J^{\text{CT}} \approx 600 \text{ cm}^{-1}$ ). By means of INDO/S-MRCI calculations, we have compared localized and delocalized electronic structures for the optimized geometry.

The optimized geometry obtained for a frozen core as described in the previous section is shown in Figure 1. We note that, in this optimization, we have kept the coordinates of the central part of the system fixed to the value of 3.6 Å observed experimentally. (There are no reliable Cu parameters available for the AM1 model.) Further refinement of the structure of the central portion was made by means of single-point INDO/S calculations, until the experimental features of the UV-vis spectrum were best reproduced. This procedure gave values of 3.76 Å for the Cu-Cu interatomic distance and 0.05 Å for the out-of-plane  $\text{O}_2$  "height". This gives the best agreement with the experimental bands and is in good agreement with the available X-ray data, as well as reported values from density

(26) Edwards, W. D.; Zerner, M. C. *Theor. Chim. Acta* **1987**, *72*, 347.

(27) Pauncz, R. *Spin Eigenfunctions*; Plenum: New York, 1979.

(28) Cory, M. G.; Zerner, M. C. *Chem. Rev.* **1991**, *91*, 813.

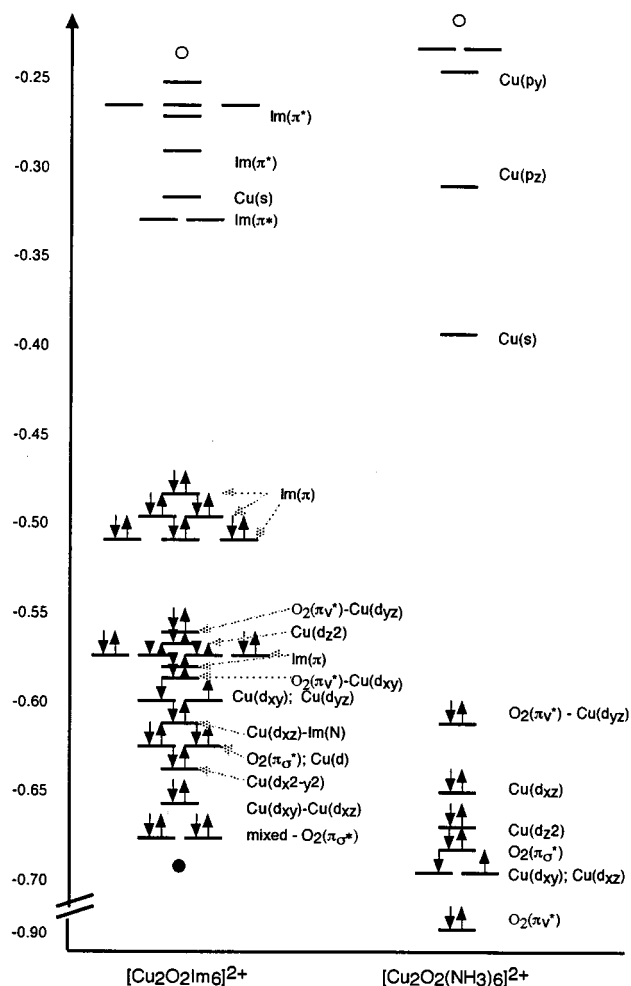


**Figure 2.** MO diagram for the complexes used to model the oxyhemocyanin molecule. Orbitals are labeled according to their largest contribution. Note that the half-filled  $\text{Cu}(d_{xz})$  orbitals (HOMO) are not the highest of the occupied orbitals in orbital energy. This is a consequence of the failure of the open-shell orbitals to obey Koopman's approximation and a failure of Koopman's approximation, in general, for MOs localized on d orbitals.

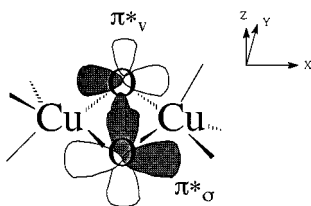


**Figure 3.** Diagram of the central portion of the oxyhemocyanin molecule, associated with the catalytic properties, showing the  $\pi$  orbitals of the peroxide bridge that are involved in the excitations.

functional calculations on the hexamino complex, varying between 3.68 and 3.82 Å, depending on the DFT model used.<sup>29</sup>

According to our calculations, the degenerate (half-filled) SOMO in the AF state is composed mainly of in-plane  $d_{xy}$  Cu orbitals, with some contribution of the  $d_{yz}$  (Figure 2). Peroxide has a degenerate set of  $\pi$  valence orbitals (the  $2p\pi^*$  responsible for the paramagnetism of  $\text{O}_2$ ), which splits in energy upon binding to the copper atoms. After Solomon,<sup>9</sup> we have named the in-plane,  $\sigma$ -bonding orbital  $\pi^*_\sigma$  and the out-of-the-plane,  $\pi$ -bonding one  $\pi^*_v$  (Figure 3). The  $\pi^*_v$  orbital of the peroxide partially mixes with the Cu  $d_{yz}$  and, to a lesser extent, with the

**Table 1.** Examination of the Magnetic Properties of the Model Oxyhemocyanin Complex of Figure 1 Using Projected Unrestricted Hartree–Fock Theory (PUHF)

	$S_z$	weight	energy (hartrees)
Weight and Energy for the $S_z = 0.00$			
Spin Components of the UHF Wave Function			
a	0.00	0.34255666	-339.424854
b	1.00	0.45202175	-339.382108
c	2.00	0.16946218	-339.313114
d		unprojected $\langle S^2 \rangle = 2.386659$	
e		$E(\text{UHF}) = -339.379252$ hartrees	
Weight and Energy for the $S_z = 1.00$			
Spin Components of the UHF Wave Function			
f	1.00	0.70198551	-339.391004
g	2.00	0.24792497	-339.318271
h	3.00	0.04482202	-339.234739
i		unprojected $\langle S^2 \rangle = 3.538626$	
j		$E(\text{UHF}) = 339.36462023$ hartrees	
Summary of Results			
${}^3E-{}^1E$			
		$E(e)-E(i) = 3211 \text{ cm}^{-1}$	UHF
		$E(b)-E(a) = 9381 \text{ cm}^{-1}$	from the $S_z = 0$ wave function
		$E(f)-E(a) = 7429 \text{ cm}^{-1}$	from the lowest PUHF energies
		$= 6398 \text{ cm}^{-1}$	from the CI, see text

$d_{xz}$ . The  $\pi^*_\sigma$  orbital, on the other hand, splits in two through mixing with the  $d_{xy}$  and  $d_{yz}$  orbitals localized on each of the copper atoms. This splitting increases as the Cu atoms approach one another and get closer, hence, to the oxygen atoms. Mixing with the d orbitals is also reflected in a stabilization of the  $\pi^*_\sigma$  orbitals. The  $\pi^*_\sigma-d_{xy}$  becomes more stable than the  $\pi^*_\sigma-d_{yz}$  due to its larger overlap (Figure 2). This effect is also larger for the shorter copper–copper distances. The calculated SOMO for the delocalized state has the same symmetry but is delocalized over the two copper centers.

Our calculations reproduce the higher stability of the AF state, with the singlet more stable than the triplet by  $6398 \text{ cm}^{-1}$ . The closed-shell, delocalized structure is  $9381 \text{ cm}^{-1}$  higher in energy than our calculated ground state.

We examine the question of magnetism a little further in Table 1, where we summarize the results of projected unrestricted Hartree–Fock (UHF) calculations, a level of theory that we have found particularly consistent for magnetism. The  $S_z = 0$  UHF calculation is very spin contaminated, as measured from the expectation value of  $S^2 = 2.387$ . For a singlet,  $S^2$  should be 0. The UHF wave function is only 34% singlet and has more triplet than singlet character, 45%. The UHF  $S_z = 1$  calculation is 70% triplet. Our best estimate of the triplet–singlet energy difference,  $E(\text{FM}) - E(\text{AF})$ , is  $7429 \text{ cm}^{-1}$ , to be compared with the CI result reported above (and in Table 1) of  $6398 \text{ cm}^{-1}$ , reasonably consistent values for such a large complex. Note that the difference obtained directly from the UHF calculations is too small, only  $3211 \text{ cm}^{-1}$ , a result largely caused by the large amount of triplet character in the  $S_z = 0$  “singlet” UHF calculation. This splitting is, however, consistent with a value of  $2500 \text{ cm}^{-1}$ , estimated by Tuzcek and Solomon using their valence bond CI model but based on spin-unrestricted X $\alpha$  calculations.<sup>9</sup>

**3.1.b.  $\text{NH}_3$ -Based Model. Isomer A.** To compare our results with those previously reported by Solomon and co-workers, we have performed similar calculations for a smaller compound, in which the imidazole groups have been replaced by  $\text{NH}_3$  (Figure 4).

The geometry of the complex has been optimized under the same constraints previously defined for the larger molecule.

(29) Flocke, M.; Pierloot, K. *J. Phys. Chem. A* **1999**, *103*, 95.

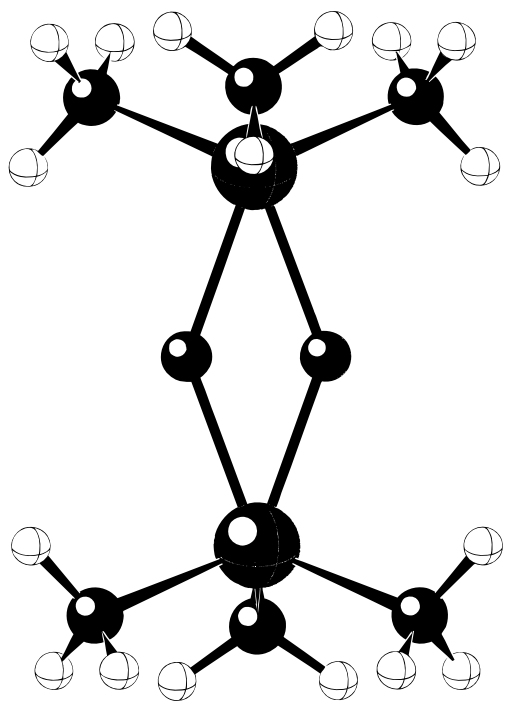


**Figure 4.** Structure of the NH<sub>3</sub>-based model derived from a constrained geometry optimization (see text).

Adjustments of the interatomic copper–copper distance and out-of-plane O<sub>2</sub> height have been also applied, yielding a Cu–Cu distance of about 3.82 Å, larger than the 3.76 Å distance we favor for the imidazole-based compound. No experimental data are available for this compound, and available DFT calculations on this complex yield distances between 3.68 and 3.82 Å, depending on the functional used for these calculations.<sup>29</sup> These distances are all larger than those observed for the oxyhemocyanin complexes, which vary between 3.56 and 3.66 Å<sup>10</sup> and, in this sense, are consistent with our requirement to increase the Cu–Cu distance in the hexamino complex to best fit the spectrum. The MO description that results for the most stable geometry is very similar to that of the imidazole complex. We have worked with a localized scheme that represents the AF coupling, defined through a degenerate SOMO composed of  $d_{xy}$  orbitals localized on each of the copper atoms. As previously described for the larger model complex, the  $\pi^*_v$  orbital also mixes with the Cu  $d_{yz}$ , whereas the  $\pi^*_\sigma$  splits and is stabilized through mixing with the copper  $d_{xy}$  and  $d_{yz}$ , resulting in two orbitals, the former more stable than the latter, due to greater overlap (Figure 2).

We calculate the AF singlet ground state 6800 cm<sup>-1</sup> lower in energy than the triplet, giving a  $2J$  value larger than the one calculated for the imidazole-based model. This, however, is quite sensitive to the geometry.

**3.1.c. Isomer B.** Regardless of the nature of the ligands, no antiferromagnetism is calculated for the ground-state structure of isomer B. We have analyzed geometries that are intermediate between those of A and B by means of variations of the Cu–Cu and O–O distances in 0.1-Å steps. We found that, for the imidazole-based model, the AF state remains the most stable one for geometries between that of complex A and the one characterized by  $r_{\text{Cu–Cu}} = 2.9$  Å,  $r_{\text{O–O}} = 2.10$  Å. For this intermediate structure, the delocalized state is still calculated 3555 cm<sup>-1</sup> higher in energy than the AF one; we have not sought the detailed geometry where these two states cross.

The MO distribution is similar in both the NH<sub>3</sub>- and the imidazole-based models, but for the contribution of imidazole-

centered orbitals in the latter that define, among others, the HOMO. The LUMO is, in both cases,  $[d_{xy}(a) + d_{xy}(b)]$ , with some asymmetric contribution of the  $p_y$  on both oxygens. The LUMO+1 is  $[d_{xy}(a) - d_{xy}(b)]$ , partially mixed in-plane with the oxygen  $p_x$  in an antibonding fashion. In the NH<sub>3</sub>-based model complex, the HOMO is centered on the  $p_z$  oxygen orbitals, partially mixed in-plane with the copper  $[d_{xz}(a) + d_{xz}(b)]$ .

### 3.1.d. Comparison with Previously Published Results.

There are no data available, in the related literature, to be compared with our results for the imidazole-based model. For the NH<sub>3</sub> model, values of 4666 and 9388 cm<sup>-1</sup> are obtained by Bernardi et al.<sup>12</sup> for the singlet–triplet splitting, from their best CASPT2 and nonlocal DFT calculations, respectively. Bérces<sup>15</sup> predicts a splitting of 3800 cm<sup>-1</sup> for this complex, based on a delocalized singlet, and a value of 6163 cm<sup>-1</sup> for the 1,4,7-triazacyclononane complex, a complex more similar to ours, and a value very consistent with our value of 6518 cm<sup>-1</sup>. Bérces's values, however, are estimated from the HOMO–LUMO gap from a ground-state description of the diamagnetism that is very different from the one we, and most others, obtain.

In relation to the B isomer, Mahapatra and co-workers<sup>16</sup> have also found fully symmetric solutions for the NH<sub>3</sub>-based complex, by means of broken symmetry single-point X $\alpha$  calculations. Ab initio RHF/STO-3G\* calculations for the same compound<sup>16</sup> predict a HOMO comprised of  $d_{x^2-y^2}$  orbitals on both copper atoms and the antisymmetric combination of  $p_y$  orbitals. This description is consistent with our calculated LUMO.

### 3.2. UV–Visible Spectroscopy. 3.2.a. Imidazole-Based

**Model Complex. Isomer A.** The UV–vis absorption spectrum of oxyhemocyanin has been examined several times using quantum methods.<sup>9,11,15</sup> As can be seen in Table 2, there are two obvious absorption bands, one in the visible (17 500–18 100 cm<sup>-1</sup>,  $\epsilon \approx 1000$  M<sup>-1</sup> cm<sup>-1</sup>) and one in the UV (29 400–30 400 cm<sup>-1</sup>,  $\epsilon \approx 20\,000$  M<sup>-1</sup> cm<sup>-1</sup>). There are also weak bands in the 700–800-nm region that are assigned to  $d \rightarrow d$  transitions of the tetragonal Cu(II). Although the ligands may have some influence, the origin of the more intense bands of the spectrum has always been associated with transitions involving the four central atoms of the oxyhemocyanin molecule,<sup>9</sup> i.e., the  $d$  orbitals on the coppers and valence orbitals of the peroxide. This assignment has been based on the fact that the bands are absent in the Met-derivative when the peroxide is removed from the binuclear cupric active site.<sup>30</sup>

From overlap and energy considerations, the high-intensity band at about 30 000 cm<sup>-1</sup> has been assigned to the  $\pi^*_\sigma \rightarrow \text{Cu(II)}$  CT transition and the low intensity band, at about 18 000 cm<sup>-1</sup>, to the  $\pi^*_v \rightarrow \text{Cu(II)}$  transition.<sup>30</sup> Our calculated spectra (Tables 2 and 3) are in good agreement with the experimental observations, but our assignment of the low-intensity bands is somewhat more complex.

As previously mentioned in section 3.1.a, the geometry of the imidazole-based complex was refined until the experimental features of the UV–vis spectrum were best reproduced (based on the positions of the first three transitions), resulting in values of 3.76 Å for the Cu–Cu interatomic distance and 0.05 Å for the out-of-plane O<sub>2</sub> “height”. Elevations of the O<sub>2</sub> between 0.0 and 1.0 Å were compared. No significant differences become evident for values between 0.1 and 1.0 Å. In the planar structure, on the other hand, the band at lower energy, of lower intensity, cannot be assigned to a  $\pi^*_v \rightarrow \text{Cu(II)}$  CT transition, because the  $\pi^*_v$  orbital does not overlap efficiently with the HOMO, centered on the Cu atoms. Decreasing the interatomic distance

(30) Solomon, E. I. In *Metal clusters in proteins*; Que, L., Jr, Ed.; ACS Symposium Series 372; ACS: Washington, DC, 1988.

**Table 2.** INDO/S-CI-Calculated Excited States of Oxyhemocyanin Model Complex for the Histidine Residues Represented by Imidazole Groups<sup>a</sup>

assignment	$\Delta E_{\text{calc}} (10^{-3} \text{ cm}^{-1})$			$\Delta E_{\text{exp}} (10^{-3} \text{ cm}^{-1})^b$
	$r_{\text{Cu-Cu}} = 3.56 \text{ \AA}$	$r_{\text{Cu-Cu}} = 3.76 \text{ \AA}$	$r_{\text{Cu-Cu}} = 3.86 \text{ \AA}$	
[2] d $\rightarrow$ d	18.3 (0.004)	15.0 (0.003)	13.3 (0.002)	14.3–15.0 (v wk)
[6] ( $\pi_v - d_{yz}^*$ , $\pi\sigma - d_{yz}^*$ )	21.3 (0.006)	17.8 (0.010)	16.3 (0.011)	17.5–18.1 (wk)
$\rightarrow$ SOMO	22.1 (0.021)	18.3 (0.013)	16.7 (0.011)	
[6] $\pi^* \rightarrow \pi^*$		25.3 (0.0001)	24.3 (0.0002)	23.5–23.6 (v wk)
[6] $\pi\sigma - d_{xy}^* \rightarrow$ SOMO	39.9 (0.198)	36.3 (0.205)	34.7 (0.407)	29.4–30.4 (m)

<sup>a</sup> Results of the calculations are shown for three different Cu–Cu distances. The numbers in brackets give the number of transitions calculated in these energy regions that have separations of less than 500  $\text{cm}^{-1}$ . In each group, only the most intense transitions are shown. The oscillator strengths are shown in parentheses. Results are from small exploratory SCF/CI calculations.

**Table 3.** Detailed Calculated Spectrum of the Oxyhemocyanin Model Complex for the Histidine Residues Represented by Imidazole Groups (Parent Compound)<sup>a</sup>

parent compound		neutral compound		experiment
no. in group	transition energy (1000 $\text{cm}^{-1}$ )	no. in group	transition energy (1000 $\text{cm}^{-1}$ )	
2	13.9, 14.6 (0.003)	2	15.4, 15.9 (0.005)	14.3–15.0 (v wk)
4	18.6–19.2 (0.030)	6	17.4–18.9 (0.018)	17.5–18.1 (wk)
2	20.2, 20.4 (0.000)			
6	22.6–23.1 (0.001)	12	25.9–29. (0.0003)	23.5–23.6 (v wk)
6	27.1–27.3 (0.001)	1	30.7 ((0.0132)	29.4–30.4 (m)
7	35.5–38.8	1	32.3 (0.0007)	
		1	34.4 (0.051)	
		1	34.8 (0.027)	
		1	36.4 (0.0003)	
		1	36.9 (0.002)	

<sup>a</sup> The neutral compound has two opposite ionized histidine groups. The numbers in parentheses are the *total* oscillator strengths in each group. Transitions within 500  $\text{cm}^{-1}$  from the next are grouped. Results are from the large CI calculation, see text.

between the copper atoms results in transition energies that are higher than the experimental values.

We will refer, in our discussion, to the spectra derived from the larger CI calculations based on the structure associated with the previously given Cu interatomic distances and oxygen atoms height reported in Table 3. The differences with other related geometries will be pointed out below.

In agreement with other authors,<sup>9</sup> our calculations indicate that the first eight transitions involve promotion of an electron into the SOMO. The first two, calculated at 13 900 and 14 400  $\text{cm}^{-1}$ , have a total calculated oscillator strength of 0.003, mostly in the upper component, to be compared with the experimental value of a broad weak feature reported from 14 300 to 15 000  $\text{cm}^{-1}$ . This is mostly Cu(d)  $\rightarrow$  SOMO. The next six calculated transitions are a mixture of  $\pi^*_{\sigma} \rightarrow$  SOMO,  $\pi^*_v \rightarrow$  SOMO CT transitions and Im( $\pi$ )  $\rightarrow$  SOMO, and they break into a group of four, calculated between 18 600 and 19 200  $\text{cm}^{-1}$ , with calculated oscillator strength of 0.030, and a group of two, calculated at 20 200 and 20 400  $\text{cm}^{-1}$ . We assume that transitions calculated within  $\sim 500$ –600  $\text{cm}^{-1}$  will not be resolved, and we therefore group them in our discussion. This lower group of four, with more  $\pi^*_{\sigma} \rightarrow$  SOMO,  $\pi^*_v \rightarrow$  SOMO CT contributions, we associate with the observed features between 17 500 and 18 100  $\text{cm}^{-1}$ . We now calculate a band of six transitions between 22 600 and 23 100  $\text{cm}^{-1}$  (0.001) which we associate with the very weak feature observed at about 23 500  $\text{cm}^{-1}$ . The number in parentheses is the calculated oscillator strength. These transitions are mostly Im( $\pi$ )  $\rightarrow$  Im( $\pi^*$ ). These transitions are considerably below those in imidazole itself and most likely stem from the triplets of the imidazoles that couple with the low-lying triplet of the complex, yielding a singlet.<sup>28</sup> The six calculated transitions between 27 100 and 27 300  $\text{cm}^{-1}$  (0.001) are of the same nature. They may be associated with the

band observed between 29 400 and 30 400  $\text{cm}^{-1}$ , but the calculated oscillator strength seems too small. Between 35 500 and 38 800  $\text{cm}^{-1}$  we calculate seven transitions, mostly combinations of the singlet Im( $\pi$ )  $\rightarrow$  Im( $\pi^*$ ) and the very intense SOMO  $\rightarrow$  SOMO state: that is, the ground state is mostly  $|\dots S_a^1 S_b^1|$ , and this latter state is mostly  $|\dots S_a^2| + |\dots S_b^2|/2^{1/2}$ . If we associate the observed feature with these transitions, then our calculated transitions are too high by 6000  $\text{cm}^{-1}$ , a large error for the INDO/S Hamiltonian for transitions that are imidazole based, implementing an error in the calculated SOMO  $\rightarrow$  SOMO transition. This seems to be confirmed on our studies of the amino complex, as shown below.

In light of the assignments previously given, the dependence of the calculated spectrum on the geometric parameters is easily understood:

(i) For the planar geometry, the  $\pi^*_v$  orbital does not overlap with the in-plane  $d_{xy}$  SOMO. Thence, the band at lower energy does not have  $\pi^*_v \rightarrow$  Cu(II) character but is assigned to the transition  $\pi^*_{\sigma} - d_{yz} \rightarrow$  Cu(II). It would have no calculated oscillator strength.

(ii) Closer distances between the Cu atoms result in calculated bands too high in energy, due to an overstabilization of the  $\pi^*_{\sigma}$  orbital through mixing with the d orbitals (see description of the orbitals, section 3.1.a, Table 2).

Inspection of the results of Table 2 shows that we obtain good agreement with the experimental data for a Cu–Cu distance = 3.76  $\text{\AA}$ , which increases our confidence in the assignments. The largest discrepancy involves the high-energy feature, which we calculate 6000  $\text{cm}^{-1}$  higher in energy than the experimental value, assuming that this is associated with the singlet Im( $\pi$ )  $\rightarrow$  Im( $\pi^*$ ) and the very intense SOMO  $\rightarrow$  SOMO state. This transition is strongly influenced by the local geometry of the central portion of the molecule (Table 2), and it might also be somewhat sensitive to the nature of the chelating ligands, which we examine below. Our calculated value is, however, substantially better, when compared with experiment, than are previous results based on a valence bond configuration interaction theory that corrects X $\alpha$  DFT calculations. We agree with these previous calculations in the importance of the strong delocalization of the electron density toward the copper centers via the in-plane  $\pi^*_{\sigma}$  orbital for the determination of the structural and electronic characteristics of the binuclear copper site of oxyhemocyanin. Delocalization leads to strong mixing of the peroxide and the d orbitals of the Cu atoms. This effect is sensitive to the geometry of the complex; adjusting the geometry to better reproduce the experimental features of the UV–vis spectrum also sheds light on the geometry of the system. In this way, the butterfly distortion (geometric distortion away from the effective  $C_{2h}$  symmetry), the interatomic distance between the Cu atoms, and even the AF coupling have been confirmed. Moreover, spectroscopic variations between the different oxyhemocyanin species have been experimentally noted<sup>31</sup> and

**Table 4.** INDO/S-CI-Calculated Excited States of Oxyhemocyanin Model Complex for the Histidine Residues Represented by NH<sub>3</sub> Groups<sup>a</sup>

assignment	$\Delta E_{\text{exp}} (10^{-3} \text{ cm}^{-1})$			$\Delta E_{\text{exp}} (10^{-3} \text{ cm}^{-1})^b$
	$r_{\text{Cu-Cu}} = 3.66 \text{ \AA}$	$r_{\text{Cu-Cu}} = 3.82 \text{ \AA}$	$r_{\text{Cu-Cu}} = 3.98 \text{ \AA}$	
[2] d $\rightarrow$ SOMO	16.8 (0.003)	14.7 (0.003)	12.4 (0.002)	14.3–15.0 (v wk)
[6] ( $\pi_v - d^*_{yz}, \pi_\sigma - d^*_{yz}$ )	21.0 (0.014)	19.1 (0.017)	17.0 (0.021)	17.5–18.1 (wk)
$\rightarrow$ SUMO	21.5 (0.018)	19.6 (0.014)	17.5 (0.010)	
[6] $\pi_\sigma - d^*_{xy}$	36.6 (0.701)	34.3 (0.612)	31.5 (0.507)	29.4–30.4 (m)
$\rightarrow$ SUMO				
[6] $\pi^*_v \rightarrow$ SUMO	38.8 (0.068)	35.9 (0.094)	32.65 (0.128)	

<sup>a</sup> Results of the calculations are shown for three different Cu–Cu distances. The numbers in brackets give the number of transitions calculated in these energy regions that have separations of less than 500 cm<sup>-1</sup>. <sup>b</sup> See ref 9.

interpreted on the basis of the relative importance of the butterfly distortion. Among them, the high-intensity band shifts to higher energy along the sequence *Busycon canaliculatum* (mollusk), *Limulus polyphemus* (arthropod), and *Cancer borealis* (arthropod).<sup>9</sup> We could also associate this shift with structural changes that might be related to the butterfly distortion but might also imply variations of the interatomic Cu–Cu distance,<sup>32</sup> as suggested in Table 2. This shift might also be a consequence of the differing ligands and differing protein environment, features difficult to examine in detail.

Addressing this latter point, and being somewhat uncomfortable about a prediction calculated some 6000 cm<sup>-1</sup> too high in energy,<sup>33</sup> we examine the influence of the ligand by deprotonating two opposite imidazoles, creating a “neutral complex”, and leaving the geometry intact. The results of this exploratory calculation also appear in Table 3. There is very little effect on the three lowest predictions; they are still in excellent agreement with experiment. However, the six bands predicted between 36 300 cm<sup>-1</sup> and 38 900 cm<sup>-1</sup> are now split by 6000 cm<sup>-1</sup>, with the lowest calculated at 30 700 cm<sup>-1</sup> (0.0132), also now calculated in very good agreement with experiment. We do not mean to imply by this calculation that the histidines of the relevant compounds are ionized in this fashion: they are likely not. What this does imply is a sensitivity to the bands calculated in this region to the details of the ligands and their environment.

Our results are not dependent on the size of the CI within the limits we are dealing with, neither in the energy of the bands, nor in their assignments. Moreover, we want to stress that our calculations are able to reproduce the experimental features without further help of extra corrections.

Since Bérces<sup>15</sup> has determined a delocalized reference state, we attempt to calculate the electronic spectrum assuming this as the ground state using the same geometry as for the localized one. Our RHF calculations yield a state similar to that described by Bérces. Although the CI yields the AF 8779 cm<sup>-1</sup> below this state (using a three-reference CIS), the transition energies and oscillator strengths are estimated assuming the closed-shell delocalized reference. Two strong transitions result: one

(31) Himmelwright, R. S.; Eickman, N. C.; Lubien, C.; Solomon, E. I. *J. Am. Chem. Soc.* **1980**, *102*, 5378.

(32) According to these calculations, the strength of the O–Cu interaction is dependent not only on their mutual separation but also on the value of the resonant integrals,  $\beta$ , that enter into the INDO Hamiltonian.<sup>23–25</sup> We have used the default  $\beta$  value for both elements. Decreasing the value of the oxygen  $\beta$  from –54 to –45 eV shifts both intense bands about 2000 cm<sup>-1</sup>, resulting in a better value for the band at higher energy but a somewhat worse value for the low-energy one. Keeping the default values, we do not associate the discrepancy in the high-energy band with the parametrization, but with the influence of the biological media, which can modify either the orientation of the imidazoles or the local charge densities on the atomic centers through the formation of hydrogen bonds. We have modeled the solvent by means of the inclusion of water molecules H-bonded through the acidic hydrogens of the imidazole groups, but this model obscures the interpretation of the UV–vis spectra.

(33) Zerner, M. C. In *Reviews of Computational Chemistry*; Lipkowitz, K. B., Boyd, D. B. Eds.; VCH Publishing: New York, 1991; Vol 2, p 313.

calculated at 23 800 (0.26) and the second at 35 500 cm<sup>-1</sup> (1.31). These transitions are associated with HOMO  $\rightarrow$  LUMO; the HOMO in this case is a delocalized orbital chiefly  $[d_{xy}(a) + d_{xy}(b)]/2^{1/2}$  with some  $d_{yz}$  admixture, and the LUMO is mostly  $[d_{xy}(a) - d_{xy}(b)]/2^{1/2}$  with some oxygen  $\pi^*_\sigma$  contribution. These transitions are more metal-to-ligand, in contrast with those reflected in the spectra calculated from the AF reference, which are ligand-to-metal. Bérces estimates two transitions from his DFT calculations at energies about twice that observed. It is unfortunate that the transition energies that we calculate assuming this reference are not much different from those we calculate assuming the AF reference, and thus do not distinguish the two possible ground states. However, the calculated oscillator strengths certainly favor the AF ground state.

**3.2.b. NH<sub>3</sub>-Based Model Compound. Isomer A.** As previously mentioned, we have obtained a localized scheme that represents the AF coupling, defined through a degenerate SOMO composed of  $d_{xy}$  orbitals localized on each of the copper atoms.

The calculation of the spectrum for different interatomic Cu–Cu distances appears in Table 4. A Cu–Cu distance of about 3.82 Å gives best the experimental values. Although the spectrum seems to be also reproduced by this smaller model complex, the assignments of the bands are not exactly the same. The lower energy bands, calculated at 19 100 and 19 600 cm<sup>-1</sup>, belong to  $\pi^*_\sigma - d_{xy}, \pi^*_\sigma - d_{yz} \rightarrow$  SOMO CT transitions. The first band, calculated at 14 700 (Cu–Cu distance 3.82 Å) or 12 400 cm<sup>-1</sup> (Cu–Cu distance 3.98 Å) is assigned to d  $\rightarrow$  SOMO transitions regardless of these geometric changes. We calculate no transition in the 23 000–29 000 cm<sup>-1</sup> region, as was found in the larger complex, as these excitations involve the histidine ligands. The intense SOMO  $\rightarrow$  SOMO transition, at  $r_{\text{Cu-Cu}} = 3.82 \text{ \AA}$ , is calculated at 34 300 cm<sup>-1</sup> and likely contributes to the observed feature at 30 000 cm<sup>-1</sup>. Note the calculated sensitivity of this transition to the local geometry of the Cu–O–Cu–O moiety. Note further that this transition is calculated high in both this complex and the more biologically relevant imidazole complex, implementing either the geometry we have assumed or the theoretical model (MR/CIS) we use for the calculation.

The main difference between the model compounds concerns the position and nature of the  $\pi^*_v \rightarrow$  SOMO CT band, which is located at higher energy in the NH<sub>3</sub>-based model for the same Cu–Cu distance. In this case, there is no mixing with the  $\pi^*_\sigma \rightarrow$  SOMO band. In the imidazole model, the  $\pi^*_v$  orbital mixes with the nitrogen atoms of the axial imidazole ligands. Lowering of the  $\pi^*_v \rightarrow$  SOMO transition seems to be associated with this mixing.

We may conclude from this comparison that, although the exact assignments are dependent on the way the model compound is defined, the low-energy spectroscopic features are mainly described as CT transitions comprising the d orbitals on the copper atoms and the  $\pi$  orbitals on the peroxide.

**3.2.c. Isomer B.** The spectra of isomer B are experimentally known for an oxyhemocyanin mimic synthetic system, with 1,4,7-triazacyclononane capping ligands bonded to the copper atoms.<sup>14,16–18</sup> For this model complex, the characteristic bands around 18 000 and 30 000  $\text{cm}^{-1}$  shift to 22 314 and 30 864  $\text{cm}^{-1}$ .<sup>14,16</sup> No theoretical assignment of the spectra of isomer B is available from the related literature.

We have calculated the spectra for the  $\text{NH}_3^-$ - and imidazole-based model complexes.

In the first case, we found nearly perfect agreement with the spectrum of the oxyhemocyanin mimic in the positions of the bands. However, the band at lower energy (22 314  $\text{cm}^{-1}$ ), which is calculated at 21 856  $\text{cm}^{-1}$  and assigned to an oxygen  $\pi^*_v$  (HOMO)  $\rightarrow$  Cu( $d_{xy}$ )–O( $p_y$ )(LUMO) transition, has no calculated intensity. It can gain intensity by means of small symmetry breaking that may involve either a shift of the oxygens out of the  $xy$  plane or a movement of the Cu atoms inside it, but these distortions are not enough to reproduce the observation that both bands in the experimental spectrum of the 1,4,7-triazacyclononane complex are of similar intensity.<sup>16</sup> The band at higher energy is associated with the contribution of two transitions, calculated at 29 741 (0.016) and 29 808  $\text{cm}^{-1}$  (0.03), and assigned to oxygen  $\pi^*_v \rightarrow$  Cu( $d_{xy}$ )–O( $p_y$ )(LUMO) and oxygen  $\pi^*_v \rightarrow$  Cu( $d_{xy}$ )–O( $p_x$ )(LUMO+1) transitions, respectively.

For the imidazole-based complex, the same assignment holds for the calculated bands, although the transitions do not involve the HOMO but the HOMO–7 and HOMO–8 orbitals, as the orbitals between HOMO–6 and HOMO are centered on the imidazoles. Transitions from these orbitals to the LUMO strongly mix in the calculated bands, shifting the calculated energies almost 2000 wavenumbers. We calculate transitions at 27 843 (0.035) and 28 111  $\text{cm}^{-1}$  (0.059) that make up the higher energy band, whereas a lower energy transition is calculated at 23 984  $\text{cm}^{-1}$  (0.000). On the basis of the main contributions, these are all assigned to oxygen  $\pi^*_v \rightarrow$  LUMO transitions.

We conclude that, for this isomer, the spectroscopy is more strongly influenced by the ligands attached to the copper atoms.

The spectroscopy of isomer B is not fully understood without an interpretation of the low intensity calculated for the lowest energy band. Our experience tells us that every time the INDO/S model fails to predict the spectroscopy, there is a related unsolved structural problem.<sup>34</sup> We have found two possible reasons for the lack of intensity of this band, both based on small structural changes that may represent the actual situation in the isomer B of the oxyhemocyanin molecule, whose structure is not known. The structure of isomer B is known for the triazacyclononane mimic.

(i) First, it is of interest to know that, if we examine a smooth transition from isomer A to isomer B, the energy of the AF state is lower than that of the delocalized closed-shell case until we are within a Cu–Cu distance but 0.1 Å more separated than that observed for the B isomer of the triazacyclononane derivative ( $r_{\text{Cu–Cu}} = 2.9$  Å,  $r_{\text{O–O}} = 2.12$  Å), section 3.1.c. For this AF state, the lowest energy band, calculated at 23 374  $\text{cm}^{-1}$  and assigned to a  $\pi_v \rightarrow$  SOMO transition, has an oscillator strength of 0.008. The transitions that make up the higher energy band, calculated at 27 717 and 28 747  $\text{cm}^{-1}$ , have calculated oscillator strengths of 0.005 and 0.008, respectively. Both calculated bands are, thence, approximately of the same intensity, in agreement with the experimental findings. Antiferromagnetism of the B isomer, which can be very hard to get

**Table 5.** Comparison of Some Geometric Features of the Geometry Inferred from the Spectroscopy and That Obtained from a BLYP DFT Calculation

	model <sup>a</sup>	DFT <sup>b</sup>
Cu–Cu	3.760 Å	3.769 Å
O–O	1.412 Å	1.457 Å
Cu–N	1.953 Å $\times$ 4 2.210 Å $\times$ 2	2.021 Å $\times$ 4 2.404 Å $\times$ 2
Cu–O–Cu	138.74°	137.74°
O–Cu–O	41.15°	42.27°

<sup>a</sup> O<sub>2</sub> is 0.05 Å above Cu–Cu axis, see text. <sup>b</sup> The Cu–O–Cu–O diamond is planar. The plane has rotated with one Cu up and one down. The molecule has an inversion center with the exception of the O<sub>2</sub>.

in the calculations because of its closer energy to the delocalized state, might then be inferred from the spectroscopic data. As in the case of the A isomer, the calculated transition energies, assuming either delocalized or AF references, are not very different. The main differences are associated with the oscillator strengths.

(ii) Since we, and others, have found that there is a great sensitivity to the nature of the chelating ligands, we examine this for our imidazole model for isomer B as a second reason for why we do not get nearly equal transition probabilities for these two bands. Holding the central core fixed at the geometry observed for the triazacyclononane isomer B, but using the location of the imidazoles at the structure observed for A, instead of maintaining the Cu–N distances, lengthens the Cu–N distances by about 0.2 Å. This modification changes the ligand field on the central core, increasing the intensity of the lower energy band to 0.013, whereas those of the transitions that make up the higher energy band decrease to 0.012 and 0.033, respectively, with very little effect on the calculated transition energies. This calculation certainly demonstrates that the intensity of these bands is very dependent on the environment defined by the ligands, which is not the same in the oxyhemocyanin molecule we are dealing with and in the triazacyclononane complex, for which the spectroscopy is actually known. Unfortunately, the spectrum of the oxyhemocyanin molecule is not known for isomer B, so this remains a prediction.

#### 4. Conclusions

We have examined the electronic and structural characteristics of oxyhemocyanin, focusing our attention on the determination of those features that are needed to reproduce the observed experimental UV–vis spectrum.

We found that the dominant bands of the spectrum originate from transitions comprising mostly the copper atoms and the peroxide through which they are bonded,  $[\text{O}_2]^{2-} \rightarrow$  Cu(II) CT transitions, and, in addition, transitions between the localized half-filled metal-based (SOMO) orbitals. The local geometry of the central part of the molecule can be determined from the calculated energy of the excitations. The calculated transition energies are in good agreement with experiment.

From the assignment of the experimentally observed transitions, we conclude that the electronic and structural characteristics of the active center of the oxyhemocyanin molecule, in isomer A, are mainly related to the following:

(i) *Antiferromagnetic coupling of the Cu atoms*, which, in a Cu(II) state, are bonded through a peroxide bridge.

(ii) Efficient interaction of the  $\pi^*$  orbitals of the peroxide with the  $d_{xy}$ ,  $d_{yz}$  on the Cu atoms. The strength of the interaction depends on the Cu–Cu and Cu–O distances. According to our calculations, the central portion of the molecule is characterized by Cu–Cu distances around 3.76 Å, and an out-of-plane shift

(34) Stavrev, K. K.; Zerner, M. C.; Meyer, T. J. *J. Am. Chem. Soc.* **1995**, *117*, 8684.



**Table 6.** Calculated Spectrum for the Model Compound Compared with That Obtained from BLYP<sup>a</sup>

INDO/s//model		INDO/s//BLYP		
no. in group	transition energy	no. in group	transition energy	comments
2	13.9, 14.6 (0.003)	2	13.2, 13.7 (0.003)	(Cu, Im( $\pi$ ) $\rightarrow$ SUMO)
4	18.6–19.2 (0.038)	6	15.0–16.9 (0.001)	( $\pi_v$ -d $^*_{yz}$ , $\pi_\sigma$ -d $^*_{yz}$ , Im( $\pi$ )) $\rightarrow$ SUMO
2	20.2, 20.4 (0.000)			Im( $\pi$ ) $\rightarrow$ Im( $\pi^*$ )
6	22.6–23.1 (0.001)	6	23.9–25.0 (0.0000)	Im( $\pi$ ) $\rightarrow$ Im( $\pi^*$ )
6	27.1–27.3 (0.001)	6	28.6–28.8 (0.0002)	Im( $\pi$ ) $\rightarrow$ Im( $\pi^*$ )
1	35.5 (0.486)	1	38.4 (0.479)	SUMO $\rightarrow$ SUMO
6	37.1–38.8 (0.156)	6	36.2–37.1 (0.073)	SUMO $\rightarrow$ Im( $\pi^*$ )

<sup>a</sup> The values are in 1000 cm<sup>-1</sup>. The members in the group are separated by less than 500 cm<sup>-1</sup>. The total oscillator strength of the group is given in parentheses.

of the peroxide group, as described by Solomon<sup>18</sup> as a butterfly distortion, is required for a proper account of the interactions.

For isomer B, on the other hand, the nature of the capping ligands seems to become more relevant for the determination of the position and intensity of the bands in the UV–visible spectrum. Although we calculate a closed-shell diamagnetic state as lowest in energy for this isomer, either AF is required to correctly reproduce the intensities, or considerable distortions of the ligand environment from that of isomer A are predicted.

The calculations have demonstrated their applicability for the definition of the structural and electronic characteristics of the active site of oxyhemocyanin through the study of the UV–visible spectrum of the complex. This information becomes of great importance because minor structural changes that are observed between different species (mollusks, arthropods) influence the catalytic activity.

#### Notes Added in the Editorial Review Process:

One of the reviewers of this paper suggested that geometry information could not be obtained through fitting spectra in the fashion that we delineate above. We have had considerable experience in doing just that,<sup>35</sup> since the determination of the N–N bond length in pyridazine in 1973,<sup>23</sup> based upon poor agreement using the reported (at that time) bond length of 1.24 Å. Others have reported similar sensitivity.<sup>36</sup>

Based on these comments, however, we have performed nonlocal density functional calculations using the BLYP functionals and the program Turbomol on the imidazole model complex. These calculations required 6 weeks on the SGI O2 (as opposed to the small spectral calculations that are of the order of 5 min). A comparison of the geometry obtained with

(35) Zerner, M. C. On Calculating the Electronic Spectroscopy of Very Large Systems. In *Problem Solving in Computational Molecular Sciences*; Wilson, S., Diercksen, G. H., Eds.; NATO ASI Series: Dordrecht, 1997.

that inferred from the spectroscopy is given in Table 5. It is interesting to note that (1) the Cu–Cu distance is the same as that inferred from the low-lying spectrum, (2) the DFT calculation has twisted the Cu–O–Cu–O plane around the O<sub>2</sub> axis in such a fashion that the molecule now has nearly an inversion center, and (3) the Cu–N distances are all slightly expanded. With respect to this latter observation, we remark that the in vivo protein of oxyhemocyanin might place restrictions on these metal–ligand distances. The model compound uses the geometries reported experimentally, as described above. We further caution that the different DFT functionals might lead to a considerable difference in Cu–Cu distances, as reported for the hexaamino complex.<sup>29</sup>

The spectroscopy predicted using the DFT geometry is compared with that of our model compound in Table 6. These two predicted spectra are remarkably similar. Before concluding, we again observe that the low-lying spectrum can, indeed, be used to infer geometry, this now becoming one more example.

**Acknowledgment.** This work was supported in part through a grant from the U.S. Office of Naval Research. Computations were aided through an IBM SUR Grant. G.L.E. is a member of the Consejo Nacional de Investigaciones Científicas y Técnicas (CONICET). This work was also partially supported by CONICET (Argentina) and by grants from the Universidad Nacional de La Plata (Argentina).

JA971231H

(36) (a) J. McKelvey (Kodak) reports on the prediction of 40 dyes using geometries obtained from experiment (0.94), BLYP (0.95), HF 6-31G\* (0.81), and AM1 (0.60), where the numbers in parentheses are the linear *R*<sup>2</sup> coefficients. Private communication. (b) George Purvis (Oxford Molecular), at the 1998 Sanibel Symposia in theoretical chemistry, reported the results of spectroscopic calculations on a series of molecules using INDO/S from CAChe which showed little correlation with experiment unless very good geometries were used.